MOLECULAR AND CELLULAR BIOLOGY, Dec. 1997, p. 7248–7259 Vol. 17, No. 12
0270-7306/97/$04.00+0

A Role for Cyclin D3 in the Endomitotic Cell Cycle

JEFFREY M. ZIMMET,[1] DANIEL LADD,[1] CARL W. JACKSON,[2] PAULA E. STENBERG,[3] AND KATYA RAVID[1,4]*

Departments of Biochemistry and Pharmacology[1] and Whittaker Cardiovascular Institute,[4] Boston University School of Medicine, Boston, Massachusetts 02118; Division of Experimental Hematology, St. Jude Children's Research Hospital, Memphis, Tennessee 38105[2]; and Department of Pathology, Oregon Health Sciences University, Portland, Oregon 97201[3]

Received 9 June 1997/Accepted 16 September 1997

Platelets, essential for thrombosis and hemostasis, develop from polyploid megakaryocytes which undergo endomitosis. During this cell cycle, cells experience abrogated mitosis and reenter a phase of DNA synthesis, thus leading to endomitosis. In the search for regulators of the endomitotic cell cycle, we have identified cyclin D3 as an important regulatory factor. Of the D-type cyclins, cyclin D3 is present at high levels in megakaryocytes undergoing endomitosis and is markedly upregulated following exposure to the proliferation-, maturation-, and ploidy-promoting factor, Mpl ligand. Transgenic mice in which cyclin D3 is overexpressed in the platelet lineage display a striking increase in endomitosis, similar to changes seen following Mpl ligand administration to normal mice. Electron microscopy analysis revealed that unlike such treated mice, however, D3 transgenic mice show a poor development of demarcation membranes, from which platelets are believed to fragment, and no increase in platelets. Thus, while our model supports a key role for cyclin D3 in the endomitotic cell cycle, it also points to the unique role of Mpl ligand in priming megakaryocytes towards platelet fragmentation. The role of cyclin D3 in promoting endomitosis in other lineages programmed to abrogate mitosis will need further exploration.

During the process of platelet production, megakaryocytes progress through a number of discrete stages, during which different controlling elements are active (30). Early in this process, committed progenitors express specific markers and continue to proliferate within a normal mitotic cell cycle. These cells then stop dividing and undergo the process known as endomitosis, during which the complement of DNA is repeatedly doubled without nuclear division or cytokinesis. A process of cytoplasmic maturation then ensues, followed at last by shedding of platelets.

The eukaryotic cell cycle consists of alternating synthesis (S) and mitosis (M) phases separated by gaps and entails a complex system of controls and restriction points. Advancement through this cycle is driven by the phosphorylating activity of enzymes known as the cyclin-dependent kinases (CDKs), whose activity is dependent upon binding to regulatory subunits known as cyclins (31, 35). Activity of the mitosis-promoting kinase, Cdc2, requires binding to a B cyclin, while progression through G_1 phase is dependent primarily upon activation of Cdk4 or Cdk6 by one of the D-type cyclins (29). The cell cycle in endomitosis, during which megakaryocytes acquire a polyploid DNA content, is considerably less well understood. Polyploidization occurs in megakaryocytes, the platelet precursors, and in other cell types, such as vascular smooth muscle cells experiencing hypertension, and in *Drosophila* embryos (25, 30, 34). Endoreduplication in some *Drosophila* cell types is indeed associated with lack of cyclin B1 (25). It is clear, however, that in megakaryocytes this process does not involve continuous DNA synthesis but rather comprises a series of discrete S phases punctuated by gaps, during which elements of G_1, G_2, and the initial stages of M phase may occur (32, 33, 53, 56). Although cyclin B-dependent Cdc2 kinase is detectable in primary megakaryocytes and megakaryocytic cell lines (6, 56), it has been shown to be downregulated in polyploid megakaryocytic cell lines compared to diploid cells (7, 56). Since abrogation of mitosis in this cell type does not lead to cell cycle arrest, but rather the cells reenter an S phase and undergo endomitosis, we focused on exploring the role of G_1-phase cyclins in promoting endomitosis.

Recent work in our laboratory has examined the roles of various cyclins in the endomitotic process. Of the defined G_1-phase cyclins, cyclin D3 is expressed at significant levels in polyploid megakaryocytes (53). This observation has been further supported in other megakaryocytic cell lines, in which cyclin D3 and to a lesser extent D1, but not D2, are detected (7). Suppression of cyclin D3 translation with antisense oligonucleotides results in a substantial block to megakaryocyte polyploidization in culture (53). In our present study, we have shown that in vivo exposure of megakaryocytes to pegylated recombinant murine megakaryocyte growth and development factor (PEG-rmMGDF), a truncated form of Mpl ligand (2, 9, 21, 23, 26), results in substantial upregulation of cyclin D3 expression and a marginal induction of cyclin D1. Stimulation by this cytokine has a variety of effects on the megakaryocytic lineage, including enhanced proliferation of megakaryocytic progenitors, stimulation of endomitosis, and augmented cellular maturation (8, 17, 54). Given the suspected importance of cyclin D3 in megakaryocytopoiesis and its apparent induction by Mpl ligand, we wished to further investigate the role of this gene product by overexpression in an in vivo system. The transgenic mouse model that we have produced constitutively expresses the native form of cyclin D3 at high levels, specifically in the platelet lineage. The phenotype reveals a significant enhancement of endomitosis and of megakaryocyte number. This result supports a major role for cyclin D3 both in megakaryocytopoiesis and in the effects of Mpl ligand on polyploidization.

* Corresponding author. Mailing address: Biochemistry, K225, Boston University School of Medicine, 80 E. Concord St., Boston, MA 02118. Phone: (617) 638-5053. Fax: (617) 638-5054.

MATERIALS AND METHODS

Plasmid construction. The plasmid PF4MERGH (47), a pUC-based plasmid containing 1.1 kb of the platelet factor 4 (PF4) promoter followed by the myc-estrogen receptor chimera and a portion of the human growth hormone (hGH) 3′ region, was first cut at a unique *Kpn*I site at the 3′ end of the hGH sequence and ligated to a linker containing a *Not*I site. Similarly, a *Not*I linker was inserted at the unique *Nde*I site located at the 5′ end of the PF4 promoter. The MER fusion gene was then excised with *Sac*I, leaving a backbone vector containing the PF4 promoter and the hGH poly(A) tail, separated by *Sac*I cohesive ends. A linker containing *Bss*HII and *Nhe*I sites in sequence was ligated to the PF4GH backbone. The resultant plasmid was then digested with *Bss*HII and *Nhe*I. This gel-purified DNA was then ligated to the compatible ends of the 5.5-kb *Bss*HII-*Xba*I fragment of the genomic clone of murine cyclin D3 (52), which contains all five exons of the coding region down to the stop codon. The resulting plasmid, referred to as PF4D3GH, was purified on a cesium chloride gradient (41), confirmed by DNA sequencing, and subsequently digested with *Not*I to release vector sequences. The resulting 6.9-kb vector-free DNA fragment was purified from a 0.8% agarose gel with the GeneClean kit (Bio 101, Vista, Calif.) and used for the production of transgenic mice as described below.

Generation of transgenic mice. DNA was microinjected into pronuclei of one-cell FVB/N strain mouse embryos to produce transgenic mice, as described before (38). Genomic DNA was isolated from the tails of potential founder mice, digested with *Sac*I, and tested for transgene integration by Southern blot analysis using a fragment of the PF4-D3 construct as a probe (see Fig. 2A). Transgene expression was detected by reverse transcriptase PCR (RT-PCR). For this purpose, total RNA was isolated from bone marrow of transgenic and control mice with TRIzol reagent (Gibco BRL, Gaithersburg, Md.). First-strand cDNA synthesis was carried out with the Moloney murine leukemia virus RT and random primers. PCR was then performed with sense and antisense primers specific to the hGH 3′ region of the transgene, and the product was analyzed by electrophoresis on a 1% agarose gel.

Fixation and histologic analysis of tissues. Samples of sternum, femur, spleen, liver, and thymus were removed from mice immediately following sacrifice by cervical dislocation. These tissues were placed in a fixative (OptimalFix; American Histology, Lodi, Calif.) and shipped to the University of California, Davis, Transgenic Histopathology Laboratory. There, the samples were dehydrated, embedded in paraffin, sectioned at 10 μm, stained with hematoxylin and eosin, coverslipped, and presented for interpretation. The marrow contents of the femur and sternum were evaluated in three-step sections each. All of the megakaryocytes in each compartment of each of the step sections were counted with a hand-held counter.

Annexin V labeling. Labeling with annexin V (20) was performed with the Apoptosis Detection Kit (R&D Systems, Minneapolis, Minn.). Bone marrow cells were taken directly following harvest, which was performed as described before (24, 38), and treated according to the manufacturer's directions. Labeled cells were cytospun onto slides, and all recognizable large megakaryocytes were analyzed for fluorescein staining on a fluorescence microscope.

In situ hybridization. Spleens of 6- to 10-week-old FVB mice injected with either PEG-rmMGDF or vehicle were removed immediately following sacrifice 3 days postinjection and fixed in 4% paraformaldehyde overnight. Spleens from untreated transgenic and control mice were similarly fixed. All tissue samples were dehydrated in graded concentrations of ethanol, cleared in xylene, and subsequently embedded in paraffin. Sections (5 μm) were affixed to Superfrost plus slides (Fisher, Pittsburgh, Pa.) and treated as described before prior to hybridization to the appropriate ^{35}S-labeled riboprobe (48a). Signal detection was accomplished by autoradiography, and quantitation was performed by statistical analysis of numbers of silver grains present per cell, as described previously (14). Slides were stained with hematoxylin and eosin prior to analysis by both bright- and dark-field microscopy.

Acetylcholinesterase staining. Bone marrow was harvested from femurs of mice as previously described (22, 38). Megakaryocytes were identified by in situ staining for acetylcholinesterase as described before (12, 40).

Ploidy analysis and determination of megakaryocyte size and granularity. Bone marrow was collected from femurs and tibias of transgenic and control mice as described before (22, 39). Marrows from each mouse were suspended in 0.5 ml of CATCH buffer (22) and incubated for 60 min at 4°C with 4A5 monoclonal antibody ascites (5) (generous gift of Sam Burstein, University of Oklahoma Health Sciences Center). The cells were then incubated with fluorescein-conjugated goat anti-rat immunoglobulin G $(Fab')_2$ (Biosource International, Camarillo, Calif.) for 30 min at 4°C. Staining with propidium iodide was followed by determination of DNA content of 4A5 positive cells by using a statistical package on a FACScan flow cytometer (Becton Dickinson, Rutherford, N.J.), as we discussed before (47). Relative megakaryocyte size and granularity were estimated as part of the flow cytometric analysis using forward-angle light scatter and orthogonal light scatter, respectively (48).

PEG-rmMGDF injections. Single injections of PEG-rmMGDF (the murine equivalent of PEG-rHuMGDF) were carried out as described previously (1). Briefly, a stock solution of PEG-rmMGDF (630 μg/ml; generous gift of Amgen, Thousand Oaks, Calif.) was diluted with 1% normal mouse serum (NMS) in phosphate-buffered saline (PBS) immediately prior to injection. A standard dilution of PEG-rmMGDF (5.0 μg/ml; 100 μl per 10 g of body weight) was prepared and injected into each mouse via the lateral tail vein.

Flow cytometric analysis of bone marrow. Bone marrow cells were collected, stained with either rat anti-mouse CD11b (Mac-1) monoclonal antibody or rat anti-mouse TER-119 erythroid cell monoclonal antibody (both from Pharmingen, San Diego, Calif.) followed by fluorescein isothiocyanate-conjugated rabbit anti-rat immunoglobulin (Sigma, St. Louis, Mo.), and subjected to flow cytometric analysis as described before (47).

Platelet counts and mean platelet volume measurement. Blood (200 to 300 μl per sample) was drawn into a 3-μl volume of 0.5 M EDTA from the orbital sinus of each anesthetized mice by using heparinized glass capillary tubes (Fisher). Samples were prepared for manual hemacytometer counts with the Unopette system (Becton Dickinson). For platelet volume measurement, blood was collected from the orbital sinus into EDTA to a final EDTA concentration of 12.5 mM. Platelets were separated on self-generated Percoll density gradients. Percoll density medium (Pharmacia, Inc., Uppsala, Sweden) was made isotonic for mouse blood with 10× Dulbecco's PBS and then diluted with an isotonic solution of the same buffer to a 40% concentration. EDTA (5 mM) was added to the medium to prevent platelet aggregation in the gradients. Continuous density gradients were generated by centrifugation of 9-ml volumes of the diluted Percoll medium at 20,000 × *g* for 20 min at 22°C in a fixed-angle rotor. Of each blood sample, 200 μl was diluted 1:1 with Hanks' balanced salt solution, layered on top of the density gradient, and centrifuged at 1,000 × *g* for 20 min at 22°C. The portion of the gradient containing platelets was collected for mean platelet volume (MPV) measurement. MPV was determined with a Coulter particle analyzer (Model ZM with Channelyzer 256). The instrument's calibration was verified with 2.02-μm-diameter latex beads before each use. Data were accumulated on each platelet sample until a count of 2,000 was achieved in the peak channel. The samples were diluted such that the coincidence level was less than 1%. The volume distributions were analyzed as log-normal distributions.

Preparation of bone marrow and platelets for transmission electron microscopy. Bone marrow, harvested as described above, was flushed from femurs of mice with 1.5% glutaraldehyde in 100 mM sodium cacodylate buffer, pH 7.4. Dimethyl sulfoxide (2%) was added, and samples were promptly microwaved for 10 s and fixed overnight at 4°C. The marrow was rinsed in 100 mM sodium cacodylate buffer and then postfixed in 2% osmium tetroxide in 100 mM sodium cacodylate for 1.5 h. The samples were dehydrated through a series of graded ethanol, infiltrated with toluene and subsequently with resin composed of DDSA, NMA, and DMP-30 (Ted Pella, Redding, Calif.) and LX-112 (Ladd Research Industries, Burlington, Vt.), and finally embedded in the above-mentioned resin. Thin sections were cut and stained with uranyl acetate and lead citrate and viewed with a transmission electron microscope (model 301; Philips Electronic Instruments, Inc., Mahwah, N.J.).

RESULTS

Mpl ligand upregulates cyclin D3 mRNA expression in megakaryocytes in vivo. Earlier work in this laboratory and by others has demonstrated that cyclin D3, but not cyclin D2, and, at low levels, cyclin D1 are expressed in primary megakaryocytes (53) and in megakaryocytic cell lines undergoing endomitosis (56). In the present study we examined whether the proliferation- and ploidy-promoting factor, Mpl ligand, induces the expression of this cyclin in megakaryocytes. In order to determine this, we have utilized in situ hybridization, which allows for the observation of relative levels of gene expression in individual primary megakaryocytes, which are easily recognized and distinguished from other hematopoietic cells by their size and morphology. Spleens were harvested 3 days following injection with either PEG-rmMGDF or vehicle to FVB mice. Following fixation and embedding, thin sections of these hematopoietic organs were hybridized to either sense or antisense riboprobes for cyclin D3 and exposed to autoradiography emulsion. As Fig. 1 clearly shows, cyclin D3 mRNA is markedly induced in megakaryocytes from PEG-rmMGDF-treated mice (Fig. 1C and D) compared to vehicle-treated controls (Fig. 1A and B). We are also able to detect a slight increase in cyclin D1 expression in similar experiments performed with a cyclin D1 riboprobe (Fig. 1E to H). Detection of an increase in cyclin D1 message required a longer exposure time than that of cyclin D3 (15 versus 8 days). The extent of increase in cyclin D expression in PEG-rmMGDF-treated megakaryocytes was evaluated by counting grains per cell, in accordance with accepted methods (14) (described in the legend to Fig. 1). While

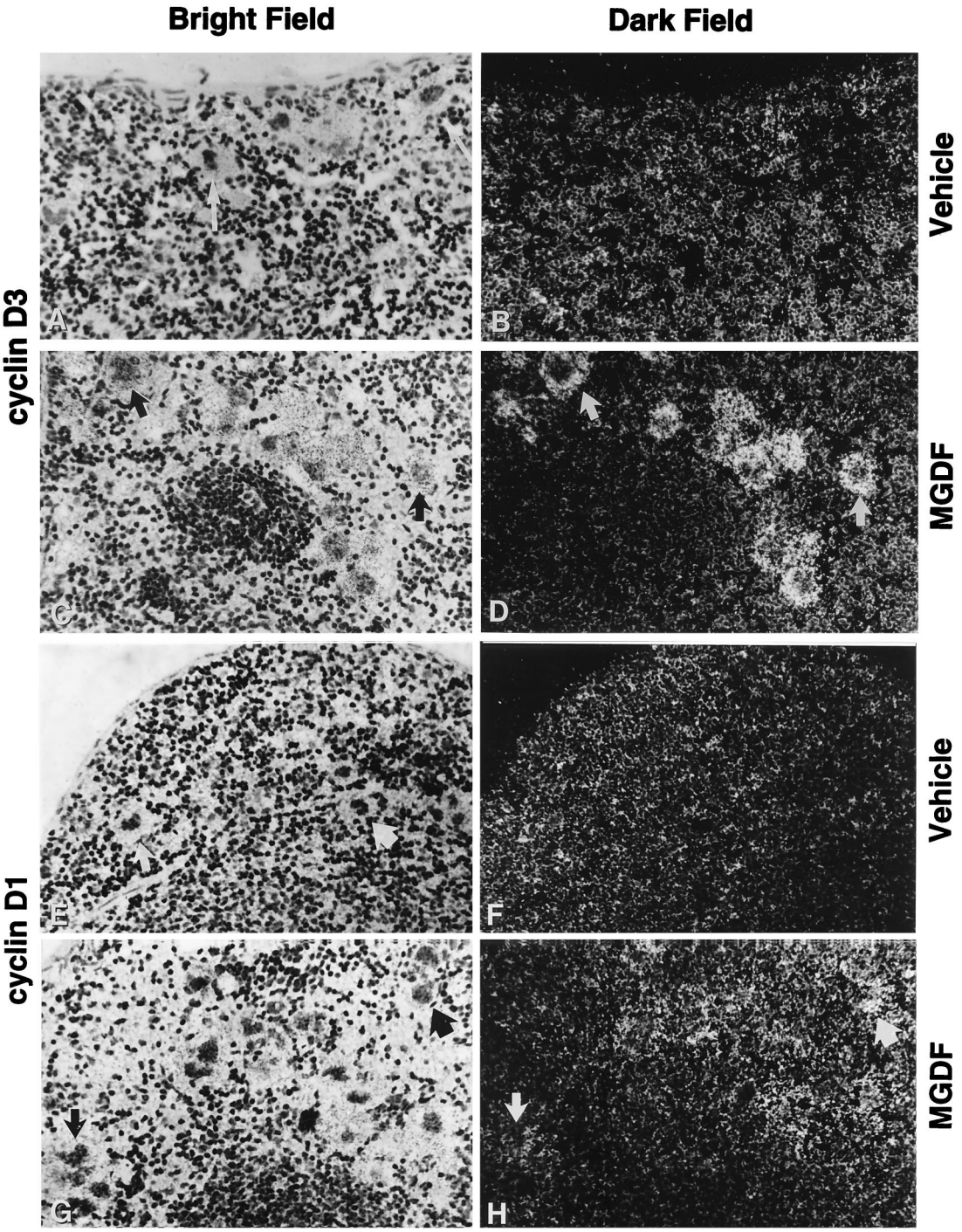

FIG. 1. Cyclin D3 is upregulated in megakaryocytes following exposure to Mpl ligand. Splenic sections from normal mice injected with PEG-rmMGDF (A, B, E, and F) or vehicle (C, D, G, and H) were hybridized to ^{35}S-labeled antisense riboprobes for cyclin D3 (A to D) or cyclin D1 (E and F). Autoradiography was performed for 8 days for cyclin D3 and for 15 days for cyclin D1. Quantitative analysis of silver grains in sections hybridized to cyclin D3 riboprobe showed an average of 83 ± 24.0 grains per megakaryocyte in vehicle-treated animals, compared to 388 ± 99.2 grains in MGDF-treated counterparts, which corresponds to a 4.7-fold induction of cyclin D3 mRNA in response to MGDF. In comparison, hybridization to cyclin D1 riboprobe resulted in an average of 127 ± 23.5 grains per vehicle-treated megakaryocyte and 204 ± 32.2 grains per vehicle-treated cell ($n = 20$), corresponding to a 1.6-fold increase. Similar experiments with sense riboprobes yielded no signal (not shown). Each experiment is represented by corresponding bright-field (A, C, E, and G) and dark-field (B, D, F, and H) light microscopic views of representative sections. Results shown are representative of three experiments, each performed with two tissue sections from each group. Arrows point to several megakaryocytes in each field. Magnification, ×140.

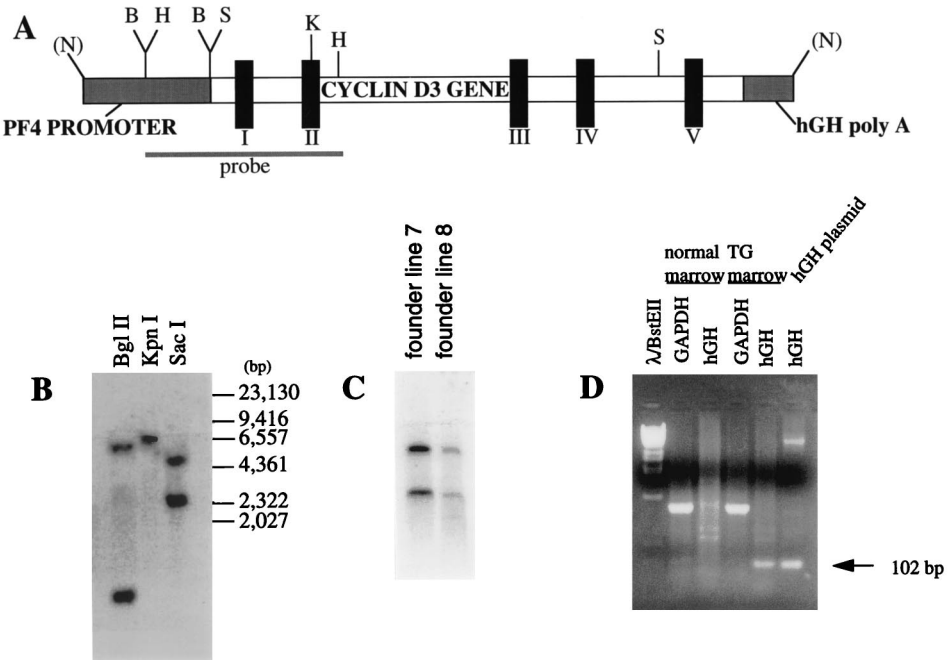

FIG. 2. Transgenic construct, representative Southern blots, and RT-PCR showing transgene expression. (A) The construct consists of 1.1 kb of the PF4 promoter linked to 5.5 kb of the murine cyclin D3 gene. The polyadenylation signal is provided by 0.3 kb of the 3′ untranslated region of the hGH gene. Black rectangles represent exons. The shaded bar represents the regions used as a probe for Southern analysis. Restriction site abbreviations: B, *Bam*HI; H, *Hin*dIII; K, *Kpn*I; N, *Not*I; S, *Sac*I. (B) Southern blot of genomic tail DNA (10 μg/lane) taken from progeny of founder 7 and founder 8 and a nontransgenic mouse and digested with *Sac*I. The copy number of the transgene integrated was estimated as 20 (line 7) and 3 (line 8), based on comparison with titrated control plasmid (not shown). The sizes of products are indicated on the right. (C) Tail DNA from founder 7 was digested with three restriction enzymes, and the Southern blot shows bands of the expected sizes. Bands and their sizes are as follows: *Bgl*II, 5.9 and 1 kb; *Kpn*I, 6.9 kb; *Sac*I, 4.6 and 2.3 kb. (D) RT-PCR showing transgene expression in bone marrow of F1 transgenic mice derived from founder 7. RNA prepared from bone marrow of control and transgenic mice was reverse transcribed and subjected to PCR using primers specific to the hGH region of the transgene. The arrow shows the expected product size. Glyceraldehyde-3-phosphate dehydrogenase (GAPDH) primers were used with each sample to verify RNA quality and fidelity of reverse transcription. TG denotes samples from transgenic mice. The *Bst*EII digest of lambda DNA (λ/BstEII) is included as a size marker. Similar results were obtained with F1 mice of transgenic line 8 (not shown).

we are aware of the limitations of in situ hybridization in making precise quantitative determinations of differences in gene expression, the striking upregulation of cyclin D3 is nonetheless clear in this case.

Generation of transgenic mice containing the PF4 promoter linked to the murine cyclin D3 gene. The results of the above-described experiment suggested that cyclin D3 may also be involved in the induction of Mpl ligand effects on polyploidization in this cell type. We therefore wished to ask the following question: to what extent can overexpression of cyclin D3 in megakaryocytes mimic Mpl ligand effects on polyploidy? In order to address this point, we have utilized 1,104 bp of the 5′ promoter region of the rat PF4 gene, which has been shown in earlier models to direct transgene expression solely in the megakaryocytic lineage (10, 38, 47), linked to the mouse cyclin D3 gene (52). The construct was tagged at the 3′ end by 0.4 kb of the hGH 3′ region, which contains a functional polyadenylation signal (Fig. 2A). The completed construct, referred to as PF4D3GH, was used for production of transgenic mice. Southern blot analysis of genomic DNA indicated that, of 33 mice produced, 2 were transgenic founders (Fig. 2B), with approximately 3 and 20 copies of transgene integrated. Digestion with different restriction enzymes indicated that the integrated transgene is not rearranged (Fig. 2C). Offspring of each of these mice inherited the transgene in a Mendelian fashion. RNA isolated from total bone marrow cells was subjected to RT-PCR using primers specific to the hGH tag of the transgene. Figure 2D shows an example of results obtained with progeny of founder 7; similar results were obtained with progeny of founder 8. The expected band is seen with RNA from bone marrow cells of transgenic but not of control mice.

Transgenic mice show a dramatic overexpression of cyclin D3 specifically in megakaryocytes. In order to confirm that we had in fact achieved overexpression of the cyclin D3 gene in megakaryocytes, splenic sections from transgenic and control mice (6 to 8 weeks old) were subjected to in situ hybridization using a ^{35}S-labeled riboprobe to murine cyclin D3. By probing for a portion of the native mRNA rather than for a unique tag on the transgene, we hoped to be able to directly compare levels of cyclin D3 mRNA in transgenic and normal mice. The extent of increase in cyclin D3 expression in megakaryocytes of transgenic mice was evaluated by counting grains per cell, in accordance with accepted methods (14) (described in the legend to Fig. 3). Morphologically recognizable megakaryocytes in spleens of control mice do show a detectable level of cyclin D3 mRNA, while megakaryocytes of transgenic mice show greater levels (Fig. 3). The experiments shown in Fig. 3 are from founder 7; similar signal intensity was seen with tissues derived from founder 8, although the copy number of transgene integrated was quite different. We thus continued analysis on heterozygote transgenic mice, which, as shown below, display a remarkable phenotype.

Megakaryocytes but not other lineages in bone marrow and spleen of transgenic mice are more numerous than those in normal counterparts. As shown in Fig. 4, histological analyses indicated that the numbers of megakaryocytes in both bone marrow and spleen of transgenic mice are dramatically increased compared to those in age-matched controls. In a con-

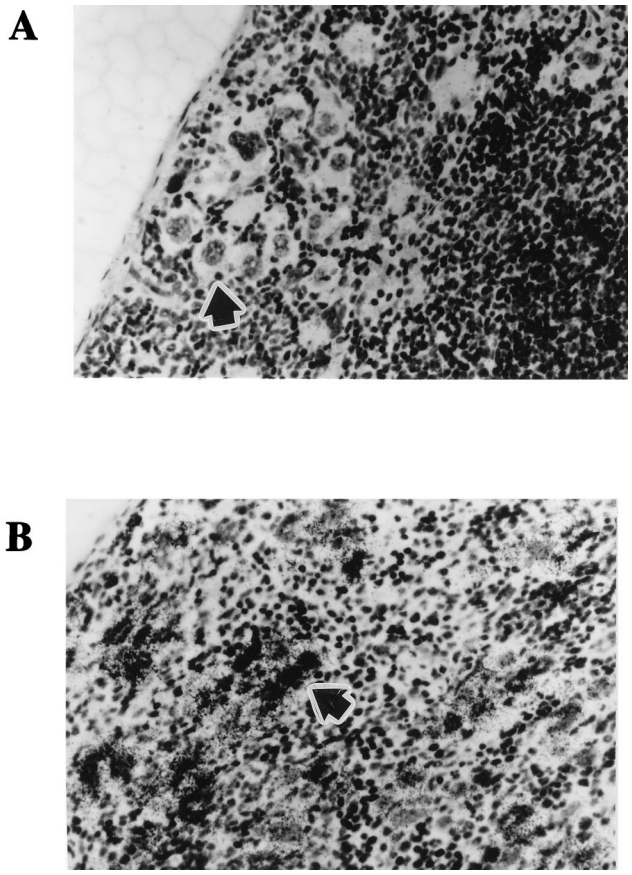

FIG. 3. Cyclin D3 is significantly overexpressed in megakaryocytes of transgenic mice. Splenic sections from control (A) and transgenic (B) mice were hybridized to an antisense riboprobe for cyclin D3. A 24-h exposure to autoradiography emulsion reveals significant cyclin D3 mRNA in transgenic megakaryocytes compared to controls. Quantitation of silver grains per megakaryocyte showed an average of 315 ± 94.1 grains per cell in transgenic animals compared to 20 ± 7.1 in controls ($n = 20$), corresponding to a 15.7-fold increase in cyclin D3 mRNA. No signal was detected in slides hybridized to a sense riboprobe for cyclin D3 (not shown). Results shown are from progeny of founder 7, although similar results were found with progeny of founder 8 (not shown). Arrows point to several megakaryocytes. Results are representative of five experiments performed. Magnification, ×160.

trol mouse of FVB strain, the average number of megakaryocytes per compartment in the sternum is 30, as we also described before (47). Cyclin D3 transgenic mice displayed a twofold increase in the number of megakaryocytes per compartment (based on three different analyses). These data were further confirmed by in situ staining for acetylcholinesterase, a unique marker for rodent and cat megakaryocytes (12), in bone marrow cells cytospun on slides. Using this assay, we have determined that, per 200,000 cytospun bone marrow cells, the number of megakaryocytes in transgenic bone marrow was 1.8-fold higher than that in controls. These data were derived from analysis of eight different slides (a total of 1.6×10^6 bone marrow cells from each group). As to the histological examination of the spleen, evaluation of five different fields (of approximately similar sizes) from each group revealed that the total number of megakaryocytes in the cyclin D3 transgenic mice was increased by 3.5-fold compared to control mice. Except for megakaryocytes, the overall cellularity of the marrow and spleen in control and transgenic animals was similar. The average weights of the spleens in age-matched control and transgenic animals were similar. Histological evaluation of a variety of other tissues showed no apparent change in nonhematopoietic systems (not shown). We also stained bone marrow cells with fluorescein-conjugated annexin V, which detects the loss of membrane asymmetry that is an early marker of apoptosis (20). By this assay, 75 transgenic bone marrow megakaryocytes and 53 controls, from 0.5×10^6 to 1×10^6 total bone marrow cells, were analyzed. The difference in labeled cells between the two groups was marginal, indicating that the increase in megakaryocyte number is not due to decreased apoptosis.

The noted increase in megakaryocyte frequency may have the potential to affect development of neighboring cells. We therefore used antibodies to lineage-specific markers to examine by flow cytometry whether the frequencies of erythroid and myelomonocytic lineages were affected by this transgene. Bone marrow cells from control and transgenic mice (progeny of founder 7) were labeled with antibody identifying erythroid cells (TER-119) or myelomonocytes (Mac-1) and subjected to flow cytometric analysis (the results are given as mean values ± standard deviations, obtained with two mice per group). Control mice showed 30.1% ± 0.8% and 25.7% ± 1.3% erythroid and myeloid cells, respectively. Transgenic mice showed 31.4% ± 0.6% and 27.4% ± 1.8% erythroid and myeloid cells, respectively. These results show that the relative numbers of cells of these lineages were not changed in bone marrows of transgenic mice versus controls. This suggests that commitment and development of other hematopoietic lineages were unaffected by the transgene.

Megakaryocytes from bone marrow of transgenic mice are larger and show an increase in DNA content similar to that seen with Mpl ligand treatment. In vivo treatment of 6- to 8-week-old mice with Mpl ligand results in both a severalfold increase in frequency of megakaryocytic cells and a significant increase in ploidy (1, 9). As seen in Fig. 5 and Table 1, megakaryocytes from cyclin D3 transgenic mice show a marked increase in DNA content, with the majority of cells reaching 32*N* and 64*N*. Comparison with mice injected with PEG-rmMGDF reveals striking similarities both in terms of ploidy distribution and megakaryocyte frequency. Relative megakaryocyte size and granularity (see Table 2) were estimated as part of the flow cytometric analysis using forward-angle scatter and orthogonal (side; 90°) light scatter, respectively (48). Transgenic megakaryocytes were significantly larger than controls as measured by this method.

Platelet number and volume are unchanged in transgenic mice. Given that both numbers and ploidy of megakaryocytes are increased in transgenic mice, one would expect a commensurate increase in platelets in the peripheral blood. Indeed, in vivo treatment of mice with Mpl ligand results in a three- to fourfold increase in circulating platelets (26, 50). Contrary to expectations, then, platelet counts in PF4D3GH mice were not significantly different from those in controls (Fig. 6A). By all appearances, platelets in these mice appear to be functional, as no mouse thus far (up to 1 year old) has suffered a bleeding diathesis and bleeding time from a standard tail biopsy does not differ from that in controls (not shown). In order to test the possibility that the larger megakaryocytes in transgenic mice yield larger rather than more-numerous platelets, we examined platelet volumes. As shown in Fig. 6B, platelet volumes in transgenic mice were not significantly different from those in controls.

In vivo treatment of transgenic mice with PEG-rmMGDF. Given the apparent connection between cyclin D3 upregulation and Mpl ligand activity, we sought to determine whether treatment with Mpl ligand could induce megakaryocytes of transgenic mice to undergo additional rounds of endomitosis.

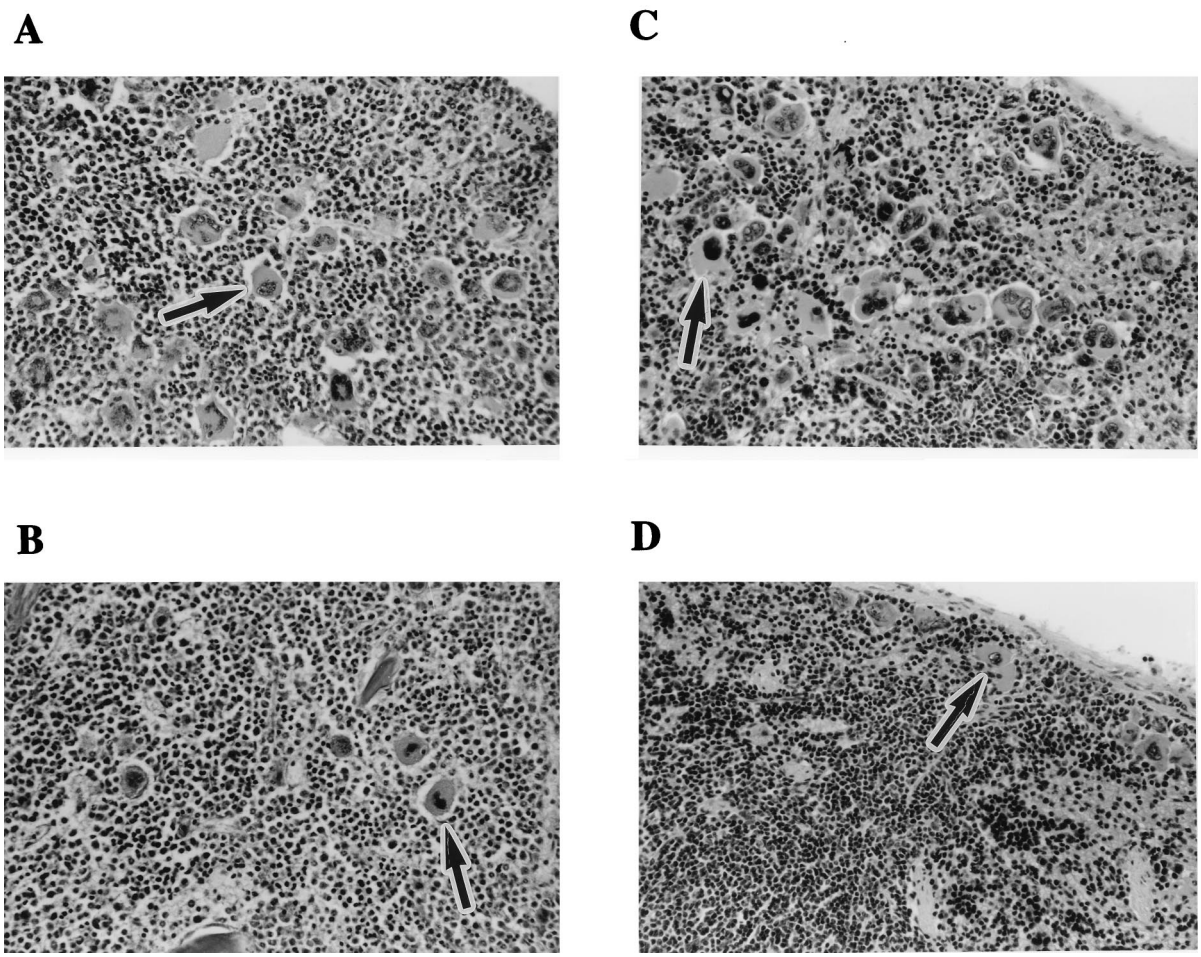

FIG. 4. Megakaryocytes are larger and more numerous in bone marrow and spleen of transgenic mice. Photomicrographs illustrate typical fields at the edge of the bone marrow in a transgenic animal (A), at the edge of the bone marrow in a control animal (B), at the edge of the spleen in a transgenic animal (the splenic capsule is at the upper right margin) (C), and at the edge of the spleen in a control animal (the splenic capsule is at the upper right margin) (D). All sections are shown at a magnification of ×160. Sections shown are from progeny of founder 7; similar results were seen with founder 8. Arrows point to several megakaryocytes recognized based on morphology.

Towards this end, we administered either PEG-rmMGDF in PBS–1% NMS or vehicle alone to transgenic and control mice by tail vein injection. As shown in Table 2, control mice treated with PEG-rmMGDF show the expected increases both in megakaryocyte ploidy and in platelet number. Transgenic mice demonstrate a higher ploidy profile than the one observed for control mice injected with PEG-rmMGDF, showing that cyclin D3 overexpression alone is sufficient to mimic most of the effects of PEG-rmMGDF on ploidy. Transgenic mice treated with PEG-rmMGDF show a further moderate increase in the percentage of highest-ploidy ($\geq$128*N*) cells. PEG-rmMGDF stimulation results in no significant increase in platelet number compared with that seen in control mice, suggesting that high levels of cyclin D3 may impede platelet development. Another measure of megakaryocytic differentiation, orthogonal light scatter, increases as cells differentiate, reflecting the increased complexity of cytoplasmic constituents, particularly the development of granules. The increase in granularity seen in controls injected with PEG-rmMGDF is not paralleled in treated transgenic mice (Table 2).

Ultrastructure of megakaryocytes and platelets of transgenic mice. Given that the larger, more numerous megakaryocytes in transgenic mice do not produce increased numbers of platelets, we sought to determine whether these cells are ultrastructurally normal or if notable maturational defects are present. The ultrastructure of transgenic bone marrow megakaryocytes was therefore compared with that of control megakaryocytes (Fig. 7A). In contrast to the majority of control megakaryocytes (75 to 95%), which exhibited well-demarcated cytoplasmic territories, the majority of transgenic megakaryocytes (75%) did not show delineation of platelet fields to the same extent, even though the demarcation membranes were distributed homogeneously throughout the cytoplasm. The demarcation membranes in these cells were not segregated from other organelles or distributed abnormally, as has been described in other models (11, 45, 46). Although a small population of the megakaryocytes from transgenic mice (approximately 25%) did contain areas of clear platelet territory delineation, indistinguishable from normal, the majority of megakaryocytes from these mice did not exhibit the "post-age stamp" appearance of control megakaryocyte cytoplasm. Granule numbers in control and transgenic megakaryocytes were comparable. A small portion (10 to 20%) of transgenic megakaryocytes exhibited secretion of alpha granule proteins into focally swollen lumena of the demarcation membrane system.

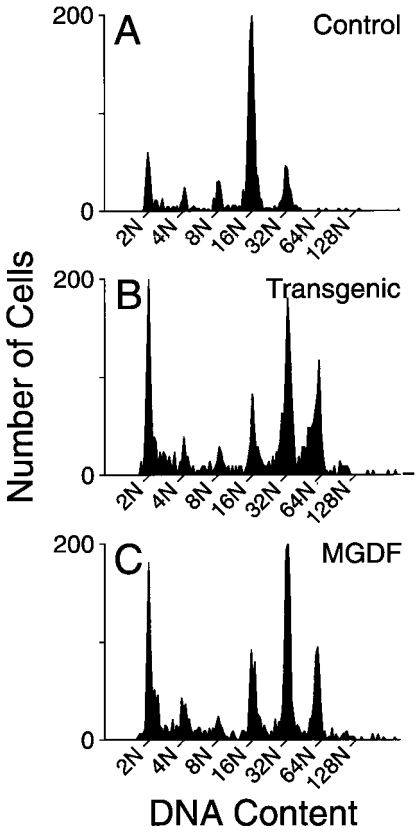

FIG. 5. Megakaryocyte ploidy distribution in transgenic mice resembles that seen in Mpl ligand-treated mice. Bone marrow cells from untreated control (A), transgenic (B), and PEG-rmMGDF-treated (C) mice were labeled with a platelet-specific antibody and subjected to fluorescence-activated cell sorter analysis following DNA staining with propidium iodide. Peaks representing each ploidy class are labeled on the *x* axis. Results are representative of four experiments performed.

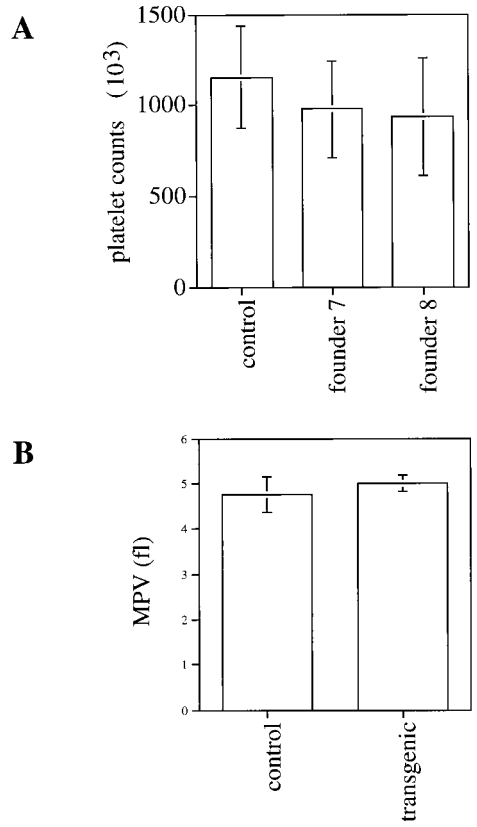

FIG. 6. Platelet number and volumes are unchanged in transgenic mice. Platelet counts (A) and volumes (B) from the peripheral blood of normal FVB/N and transgenic mice. Platelet counts shown are averages ± standard deviations (error bars) for the following numbers of mice: for the wild type (control), for 14; founder 7, 14; and for founder 8, 10. MPVs from progeny of founder 7 and from control mice were determined, and data shown represent averages ± standard deviations (error bars) for five mice.

Platelet ultrastructure and size were similar in both control and transgenic mice (Fig. 7B). Granule numbers were also comparable between these groups. Amounts and distribution of alpha granule PF4 and P selectin, as assessed by immunoelectron microscopy, were comparable between control and transgenic samples (not shown). Significantly, despite the fact that control and transgenic bone marrow samples contained different proportions of megakaryocytes with ultrastructurally distinct arrangements of demarcation membranes, platelet ultrastructure and size were normal in both groups.

DISCUSSION

The road from committed megakaryocytic progenitor to circulating platelets is complex and poorly understood. During this process, megakaryocytes progress first through a standard mitotic cell cycle and subsequently through endomitosis. The question of what regulatory elements differ between these two processes is an important one. During the mitotic cell cycle, cyclins contribute to the progression from phase to phase through interactions with their partner CDKs. The cyclin B-Cdc2 kinase, for example, controls the transition from G_2

TABLE 1. Megakaryocyte DNA content distribution in transgenic mice[a]

Mouse group	% of cells in ploidy class						
	2*N*	4*N*	8*N*	16*N*	32*N*	64*N*	128*N*
Control	13.8 ± 1	6.8 ± 0.9	12.3 ± 1.4	52.7 ± 1.4	12.5 ± 1.6	1.2 ± 0.2	0.4 ± 0.1
Line 7	21.4 ± 1.2	8.5 ± 1.1	3.0 ± 0.6	11.5 ± 0.3	31.0 ± 0.8	22.8 ± 2.6	0.6 ± 0.2
Line 8	21.6	12.5	6.7	14.8	25.1	17.4	1.9

[a] Bone marrow cells were harvested from the femurs of transgenic and control mice, labeled with antiplatelet antibody (4A5) and a secondary fluorescein isothiocyanate-labeled antibody, and stained with propidium iodide for measurement of DNA content. The results for progeny of founder 7 and those for control mice are given as percentages of megakaryocytic cells in each ploidy class, expressed as average values ± standard errors of the means for four mice. The statistical difference between groups was derived by *t* tests. The frequency of cells at ≥32*N* was significantly greater in transgenic mice ($P < 0.01$). Results for a progeny of founder 8 from a representative experiment (our of two performed) are also shown.

TABLE 2. Megakaryocyte ploidy distributions and platelet counts following in vivo MGDF treatment[a]

Mouse group	Platelet count ($10^3/\mu l$)	Mean channel no.		% of cells in ploidy class						
		Meg size ≥8*N*	Meg granularity ≥8*N*	2*N*	4*N*	8*N*	16*N*	32*N*	64*N*	128*N*
Control + vehicle	1,478 ± 158	502 ± 16	182 ± 5	19.9 ± 2.0	12.0 ± 1.6	7.3 ± 0.3	39.4 ± 2.0	17.1 ± 0.4	2.5 ± 0.5	1.7 ± 0.4
Control + MGDF	4,083 ± 251	526 ± 13	209 ± 7	24.0 ± 3.2	11.6 ± 0.5	6.0 ± 0.6	17.1 ± 2.1	26.6 ± 2.1	12.7 ± 0.9	2.0 ± 0.2
Transgenic + vehicle	1,077 ± 53	565 ± 10	180 ± 6	23.5 ± 1.2	11.8 ± 0.5	3.7 ± 0.4	11.0 ± 1.6	23.9 ± 2.2	22.2 ± 1.4	3.8 ± 0.7
Transgenic + MGDF	1,645 ± 199	569 ± 11	175 ± 7	21.3 ± 1.2	12.9 ± 0.4	5.2 ± 0.3	13.3 ± 0.8	16.0 ± 1.0	19.5 ± 1.1	11.8 ± 0.9

[a] The tail veins of transgenic (progeny of founder 7) and control mice were injected with MGDF (50 μg/kg) in PBS–1% NMS or with vehicle alone. Bone marrows were harvested and analyzed for megakaryocyte (Meg) content after 3 days, when peak effect on ploidy is seen (1). Megakaryocyte size and granularity were assessed by forward-angle light scatter and orthogonal light scatter, respectively, and expressed as mean channel numbers of the light scatter distributions as determined with the flow cytometer. Blood was collected for platelet counts 5 days postinjection, at which time the peak for this effect occurs. The results are averages ± standard errors of the means for four mice for transgenic groups and three mice for controls. The statistical differences between groups were derived by *t* tests. The increase in platelet count in transgenic mice injected with MGDF is statistically significant ($P < 0.05$). The difference in size between vehicle-injected transgenic and control mice is significant ($P < 0.01$), as is the difference between granularity of MGDF-treated transgenic mice and controls ($P < 0.02$). We noted that vehicle injection in control mice significantly increased the apparent percentage of 2*N* cells but not of cells of other ploidy classes (compared Table 1).

phase to mitosis (3). Although this kinase is detectable in primary megakaryocytes and cell lines (6, 56), it has been shown to be downregulated in polyploid megakaryocytic cell lines compared to diploid cells (7, 56). The D-type cyclins, on the other hand, are active in promoting passage through the G_1 phase (28). Of the three D-type cyclins, cyclin D3 has been found to be present at significant levels in megakaryocytes, while cyclin D1 is found in relatively lower amounts and cyclin D2 is not measurable (7, 56). The use of antisense oligonucleotides to cyclin D3 in a mouse bone marrow culture system significantly abrogated the development of polyploid megakaryocytes (53).

In the present study, we have used in situ hybridization to show that of the D-type cyclins, cyclin D3 is strongly induced following Mpl ligand stimulation of megakaryocytes. We wished to know if any of the known effects of Mpl ligand may be attributed, directly or indirectly, to the observed upregulation of cyclin D3. Could isolated overexpression of this gene reproduce some of these effects?

In order to investigate these questions, we have linked the murine cyclin D3 gene to a 1.1-kb fragment of the PF4 promoter. The PF4 gene itself is known to be expressed in early megakaryocytic progenitors (51), and our previous studies using this same fragment of the promoter have shown it to be sufficient to drive high-level, megakaryocyte-specific expression of transgenes in mice (38, 47). The results of cyclin D3 overexpression are immediately seen upon microscopic examination of hematopoietic tissues from these mice, which reveals a striking increase in both megakaryocyte frequency, more so in the spleen than in the marrow, and size. Fluorescence-activated cell sorter analysis of the DNA content of megakaryocytic cells reveals a marked increase in ploidy, with 32*N* and 64*N* cells composing a significantly increased percentage of the whole. Why is megakaryocyte number increased more in spleen than in marrow? Marrow is the primary site of hematopoiesis in rodents, although a small amount of hematopoiesis occurs in the spleens of normal mice. The marrow cavities of rodents are almost completely filled with hematopoietic cells, leaving little room for hematopoietic expansion. The spleen does not have the same size restraint, and therefore the spleen can increase hematopoiesis more than marrow when necessary. The fold increase in number of splenic megakaryocytes is usually greater than the fold increase in marrow megakaryocytes when megakaryocytopoiesis is stimulated. For instance, Ulich et al. (49), Kabaya et al. (15), and Yan et al. (55) reported that MGDF produced a larger increase in marrow megakaryocytes than in splenic megakaryocytes. Taken together, our results suggest that cyclin D3 overexpression affects both the number of megakaryocytes and the progress of endomitosis. These observations are reminiscent of Mpl ligand administration, which results in increased megakaryocyte number and enhanced endomitotic development as well as a severalfold increase in platelets (1, 9, 26, 50). While the effects of cyclin D3 or Mpl ligand on ploidy are completely indistinguishable, overexpression of cyclin D3 in cells committed to the megakaryocytic lineage (via the PF4 promoter) leads to a moderate increase in megakaryocyte number, compared to the reported effects of Mpl ligand on bone marrow cells (15, 49).

Also, unlike mice that have been administered Mpl ligand, cyclin D3 overexpression mice show unaltered levels of circulating platelets. Moreover, injection of PEG-rmMGDF to these mice results in no significant increase in platelet count, compared to a three- to fourfold increase in control mice. What is the explanation? The C3H mouse presents a similar picture, with increased ploidy (32*N* as the modal ploidy) but normal platelet count, platelet size (13), and platelet survival (27). Normal platelet survival, size, and number suggest that platelet production is ineffective in this case. Three possibilities could explain normal platelet count in the presence of increased megakaryocyte ploidy and number in the cyclin D3 overexpressing mouse. First, platelet size could be increased. We found that this was not the case. Second, platelet survival could be shortened. Third, platelet production may be ineffective. This final likely explanation suggests that cyclin D3 overexpression may in fact inhibit terminal maturation of megakaryocytes. In the normal case, perhaps cyclin D3 must be downregulated prior to platelet production. Also plausible is the idea that cyclin D3 upregulation alone is not sufficient to promote terminal megakaryocyte development and platelet production, processes for which additional Mpl ligand-induced signals must be necessary.

The ultrastructural morphology of the transgenic megakaryocytes, while not grossly aberrant, does show subtle but clear changes in the demarcation membrane system, as described above. Such changes suggest comparisons to previous transgenic mouse models. The overexpression of E2F-1 in megakaryocytes, driven by the same PF4 promoter that we use here, resulted in a low platelet count accompanied by abnormalities in both the demarcation membranes and alpha granules of megakaryocytes (10). Rather than the normal uniform distribution of membranes, E2F-1 megakaryocytes showed patchy areas of hyperdemarcation. Alpha granules, which were reduced in total number, were excluded from these regions.

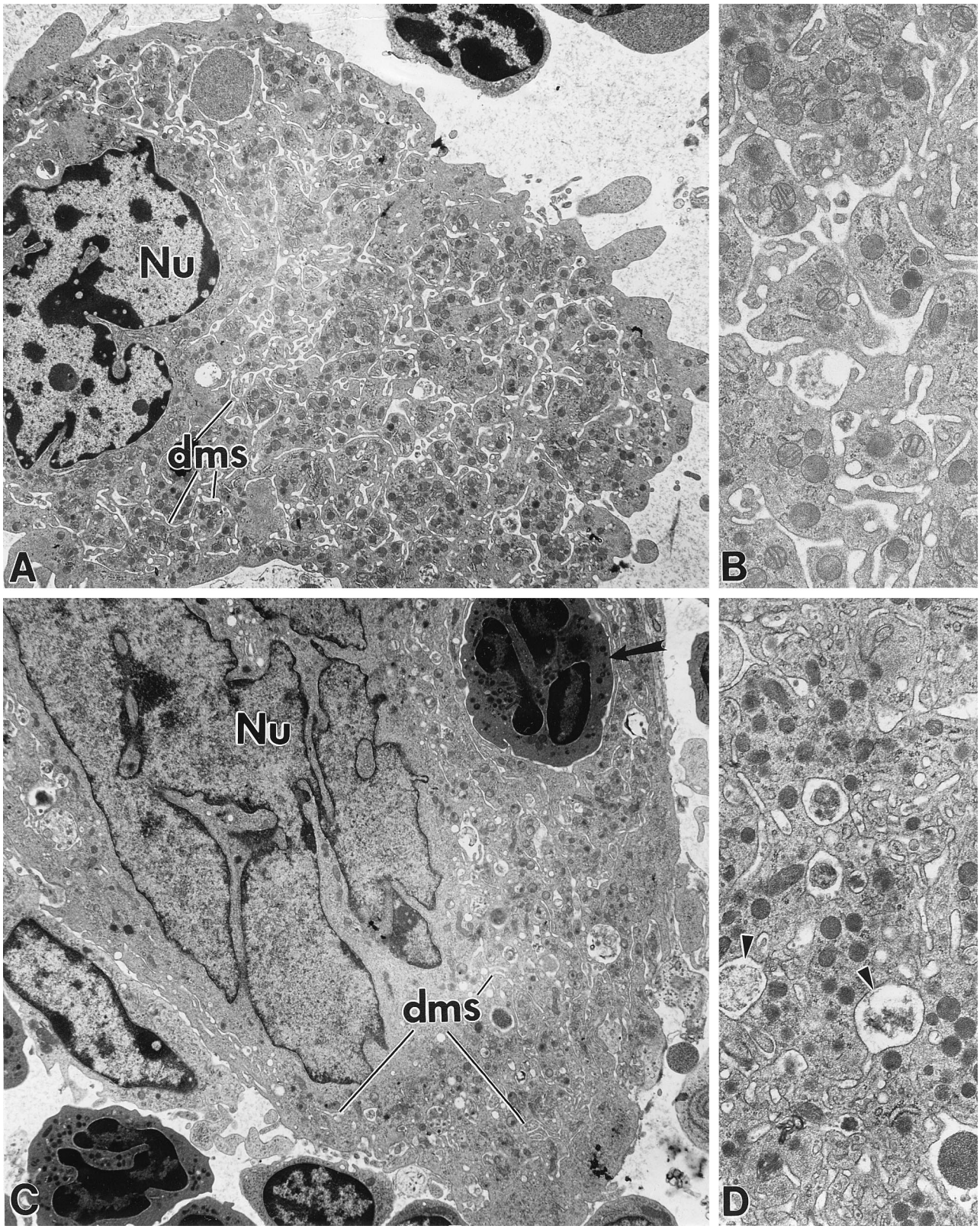

FIG. 7. Transmission electron micrographs of representative megakaryocytes and platelets from control (A, B, and E) and transgenic (C, D, and F) mice. Approximately 50 megakaryocytes from each sample were analyzed. The nucleus (Nu) and demarcation membrane system (dms) are labeled (A and C). In contrast to the well-demarcated cytoplasm shown in panel A, the dms in panel B, while homogeneously distributed in the cytoplasm, appears less well developed. Granule numbers are comparable in both cells. Panels B and D illustrate these points but at a higher magnification. (C) The arrow indicates a neutrophil which is emeripolesing through the megakaryocyte cytoplasm; (D) the arrowheads indicate focally swollen dmss that contain secreted proteinaceous material. The size, morphology, and organelle content of the transgenic (E) and control (F) platelets are comparable. Magnifications: A and B, ×5,300; C and D, ×16,000; E and F, ×9,000.

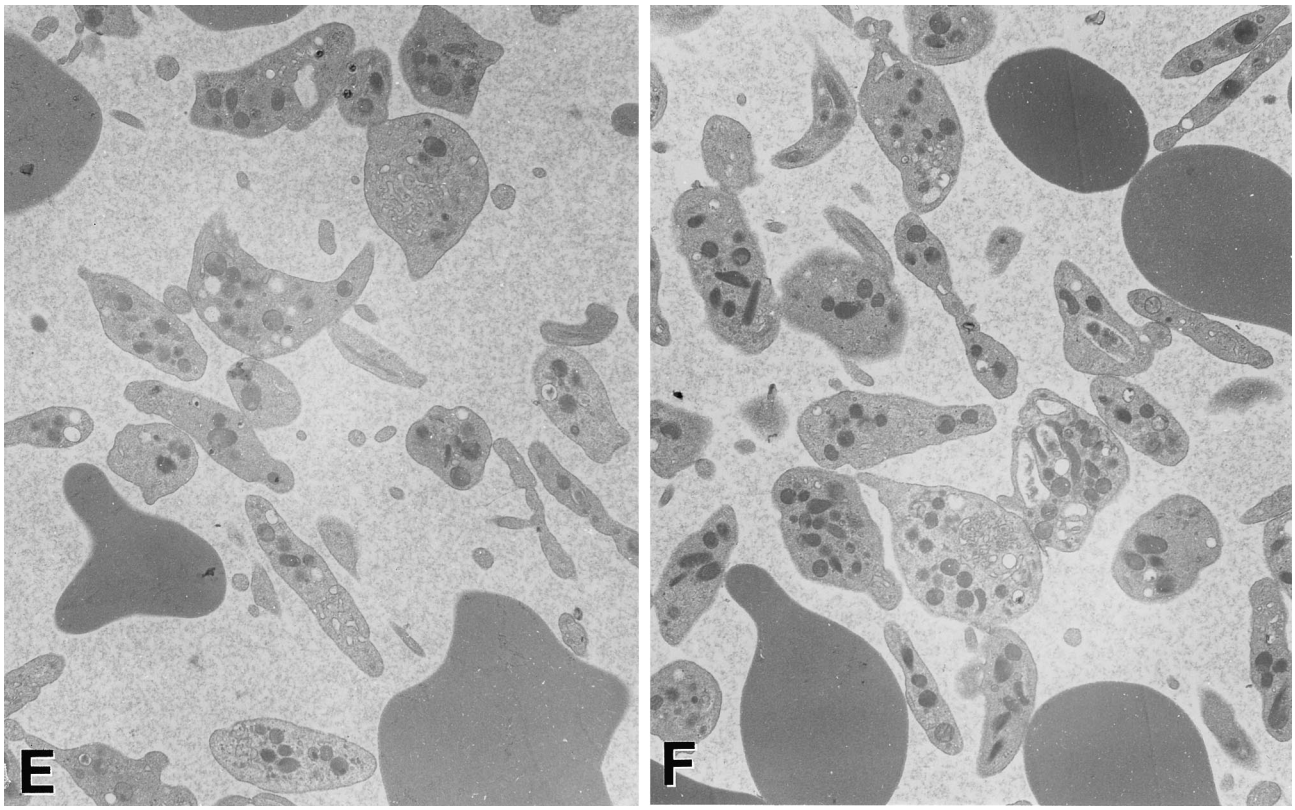

FIG. 7—*Continued.*

Similarly, megakaryocytes from mice lacking a functional transcription factor NF-E2 were seen to lack normal distribution and organization of demarcation membranes, while granules were sparse (42). These mice also presented with absolute thrombocytopenia. In contrast to these examples, cyclin D3 transgenic mice display a significantly milder phenotype. Granule frequency and distribution were normal. The demarcation membranes, while incompletely developed in the majority of cells, were relatively uniform in their distribution. Nevertheless, the reduced membrane demarcation in these cells may explain why PEG-rmMGDF was only partly effective in raising platelet counts compared to that in normal mice. Recent works argue that while Mpl ligand may be required for full megakaryocytic maturation (57), its activity does not extend to direct induction of the final stages of platelet fragmentation. An important conclusion derived from our study is that an increase in megakaryocyte ploidy and number is not sufficient to increase platelet count. While Mpl ligand may not directly stimulate the final platelet fragmentation events, it nonetheless activates a program that is permissive for such fragmentation to occur.

Several groups have described cell cycle effects of D-type cyclin overexpression. The overexpression of cyclins D1 and D2 in fibroblasts in culture, for example, resulted in increased rates of G_0-to-S- and G_1-to-S-phase transition, which in turn led to increased rates of proliferation (36). In cultured myeloid cells, D-type cyclin overexpression produced a shortening of G_1 phase, with cyclin D2- and D3-overexpressing cells displaying an inability to differentiate in response to cytokine (16). Overexpression of cyclin D1 in lymphocytes of transgenic mice, on the other hand, had no effect on cell cycle activity but hindered maturation of these cells (4). Can the phenotype of our transgenic mouse model be fully explained by the current concept of cyclin D3 activity? Most treatments of the D-type cyclins in the literature refer to these proteins essentially as interchangeable regulatory subunits of CDKs. Studies of knockout mice with null mutations in cyclin D1 or D2 have been published, and these mutations have resulted in relatively minor, focal defects (43, 44). The presumption has been that, except in tissues in which there is insufficient overlapping expression of the other family members, substitution of another D cyclin compensates completely for the deleted protein in all essential functions. Several other observations bring to light the possibility of unique roles for individual D cyclins. Of particular interest is the repeated finding that cyclin D3 is upregulated in myoblasts upon terminal differentiation to myotubes (19, 37). In the same system, cyclin D1 is predictably downregulated. The suggestion of a distinct and unique role for cyclin D3 in differentiated or differentiating cells has been offered in these reports (18). A recent study substantiates the idea that the D-type cyclins have functions wholly separate from their role as activators of CDKs. The finding that cyclin D1 stimulates estrogen receptor-mediated transcriptional activation while cyclins D2 and D3 lack this activity demonstrates conclusively that the D-type cyclins are not entirely redundant in function (58). The results of our present study indicate that cyclin D3 acts, in cells programmed to abrogate mitosis, to induce polyploidization. Although the redundancy of other D-type cyclins in this regard will require further investigation, the dramatic upregulation of only cyclin D3 by Mpl ligand suggests that this is the physiologically important regulator of endomitosis. Endoreduplication also occurs in other lineages, such as vascular smooth muscle cells exposed to hypertension and drosophila embryos (25, 34). The regulation of these cell

cycles is still poorly understood. It would be interesting, then, to explore the role of cyclin D3 or other D-type cyclins in further promoting endoreduplication in these lineages.

ACKNOWLEDGMENTS

We gratefully acknowledge Paul Toselli for assistance in tissue preparation, in situ hybridization, and microscopy; Richard Ashmun and Sam Lucas for flow cytometric analysis of megakaryocytes; Melanie White for platelet size analysis; and Robert Cardiff for histopathologic analysis of tissues. We are grateful to Robert Weinberg and Piotr Sicinski for invaluable insight and collaboration on the characterization of the cyclin D3 gene. We thank Amgen, Inc., for the generous provision of PEG-rHuMGDF.

This work was supported by NIHLBI grant HL53080 to K.R.

K.R. is an Established Investigator with the American Heart Association.

REFERENCES

1. **Arnold, J. T., N. C. Daw, P. E. Stenberg, D. Jayawardene, D. K. Srivastava, and C. W. Jackson.** 1997. A single injection of pegylated murine megakaryocyte growth and development factor (MGDF) into mice is sufficient to produce a profound stimulation of megakaryocyte frequency, size, and ploidization. Blood **89:**823–833.
2. **Bartley, T. D., J. Bogenberger, P. Hunt, Y. S. Li, H. S. Lu, F. Martin, M. S. Chang, B. Samal, J. L. Nichol, S. Swift, M. J. Johnson, R.-Y. Hsu, V. P. Parker, S. Suggs, J. D. Skrine, L. A. Merewether, C. Clogston, E. Hsu, M. M. Hokom, A. Hornkohl, E. Choi, M. Pangelinan, Y. Sun, V. Mar, J. McNinch, L. Simonet, F. Jacobsen, C. Xie, J. Shutter, H. Chute, R. Basu, L. Selander, D. Trollinger, L. Sieu, D. Padilla, G. Trail, G. Elliot, R. Izumi, T. Covey, J. Crouse, A. Garcia, W. Xu, J. Del Castillo, J. Biron, S. Cole, M. C.-T. Hu, R. Pacifici, I. Ponting, C. Saris, D. Wen, Y. P. Yung, H. Lin, and R. A. Bosselman.** 1994. Identification and cloning of a megakaryocyte growth and development factor that is a ligand for the cytokine receptor Mpl. Cell **77:**1117–1124.
3. **Blow, J. J., and P. Nurse.** 1990. A cdc2-like protein is involved in the initiation of DNA replication in Xenopus egg extracts. Cell **62:**855–862.
4. **Bodrug, S. E., B. J. Warner, M. L. Bath, G. J. Lindeman, A. W. Harris, and J. M. Adams.** 1994. Cyclin D1 transgene impedes lymphocyte maturation and collaborates in lymphomagenesis with the myc gene. EMBO J. **13:**2124–2130.
5. **Burstein, S. A., P. Friese, T. Downs, and R. L. Mei.** 1992. Characteristics of a novel rat anti-mouse platelet monoclonal antibody: application to studies of megakaryocytes. Exp. Hematol. **20:**1170–1177.
6. **Carrow, C. E., N. E. Fox, and K. Kaushansky.** 1996. Purified endomitotic megakaryocytes display a functional cyclin B1-associated mitotic kinase. Blood **88:**287a. (Abstract 1138.)
7. **Datta, N. S., J. L. Williams, J. Caldwell, A. M. Curry, E. K. Ashcraft, and M. W. Long.** 1996. Novel alterations in CDK1/cyclin B1 kinase complex formation occur during the acquisition of a polyploid DNA content. Mol. Biol. Cell **7:**209–223.
8. **Debili, N., F. Wendling, A. Katz, J. Guichard, J. Breton-Gorius, P. Hunt, and W. Vainchenker.** 1995. The Mpl-ligand or thrombopoietin or megakaryocyte growth and differentiative factor has both direct proliferative and differentiative activities on human megakaryocyte progenitors. Blood **86:**2516–2525.
9. **de Sauvage, F. J., P. E. Hass, S. D. Spencer, B. E. Malloy, A. L. Gurney, S. A. Spencer, W. C. Darbonne, W. J. Henzel, S. C. Wong, W. J. Kuang, K. J. Oles, B. Hultgren, L. A. Solberg, D. V. Goeddel, and D. L. Eaton.** 1994. Stimulation of megakaryocytopoiesis and thrombopoiesis by the c-Mpl ligand. Nature **369:**533–538.
10. **Guy, C. T., W. Zhou, S. Kaufman, and M. O. Robinson.** 1996. E2F-1 blocks terminal differentiation and causes proliferation in transgenic megakaryocytes. Mol. Cell. Biol. **16:**685–693.
11. **Hill, R. J., M. K. Warren, P. Stenberg, J. Levin, L. Corash, R. Drummond, G. Baker, F. Levin, and Y. Mok.** 1991. Stimulation of megakaryocytopoiesis in mice by human recombinant interleukin 6. Blood **77:**42–48.
12. **Jackson, C. W.** 1973. Cholinesterase as a possible marker for early cells of the megakaryocytic series. Blood **42:**413–421.
13. **Jackson, C. W., S. A. Steward, P. J. Chenaille, R. A. Ashmun, and T. P. McDonald.** 1990. An analysis of megakaryocytopoiesis in the C3H mouse: an animal model whose megakaryocytes have 32N as the modal DNA class. Blood **76:**690–696.
14. **Jonker, A., P. A. de Boer, M. J. van den Hoff, W. H. Lamers, and A. F. Moorman.** 1997. Towards quantitative in situ hybridization. J. Histochem. Cytochem. **45:**413–423.
15. **Kabaya, K., H. Akahori, K. Shibuya, Y. Nitta, M. Ida, M. Kusaka, T. Kato, and H. Miyazaki.** 1996. In vivo effects of pegylated recombinant human megakaryocyte growth and development factor on hematopoiesis in normal mice. Stem Cells **14:**651–660.
16. **Kato, J. Y., and C. J. Sherr.** 1993. Inhibition of granulocyte differentiation by G1 cyclins D2 and D3 but not D1. Proc. Natl. Acad. Sci. USA **90:**11513–11517.
17. **Kaushansky, K., S. Lok, R. D. Holly, V. C. Broudy, N. Lin, M. C. Bailey, J. W. Forstrom, M. M. Buddle, P. J. Oort, F. S. Hagen, G. J. Roth, T. Papayannopoulou, and D. C. Foster.** 1994. Promotion of megakaryocyte progenitor expansion and differentiation by the c-Mpl ligand thrombopoietin. Nature **369:**568–571.
18. **Kiess, M., R. M. Gill, and P. A. Hamel.** 1995. Expression and activity of the retinoblastoma protein (pRB)-family proteins, p107 and p130, during L6 myoblast differentiation. Cell Growth Differ. **6:**1287–1298.
19. **Kiess, M., R. M. Gill, and P. A. Hamel.** 1995. Expression of the positive regulator of cell cycle progression, cyclin D3, is induced during differentiation of myoblasts into quiescent myotubes. Oncogene **10:**159–166.
20. **Koopman, G., C. P. Reutelingsperger, G. A. Kuijten, R. M. Keehnen, S. T. Pals, and M. H. van Oers.** 1994. Annexin V for flow cytometric detection of phosphatidylserine expression on B cells undergoing apoptosis. Blood **84:**1415–1420.
21. **Kuter, D. J., D. L. Beeler, and R. D. Rosenberg.** 1994. The purification of megapoietin: a physiological regulator of megakaryocyte growth and platelet production. Proc. Natl. Acad. Sci. USA **91:**11104–11108.
22. **Kuter, D. J., S. M. Greenberg, and R. D. Rosenberg.** 1989. Analysis of megakaryocyte ploidy in rat bone marrow cultures. Blood **74:**1952–1962.
23. **Kuter, D. J., and R. D. Rosenberg.** 1994. Appearance of a megakaryocyte growth-promoting activity, megapoietin, during acute thrombocytopenia in the rabbit. Blood **84:**1464–1472.
24. **Kuter, D. J., and R. D. Rosenberg.** 1990. Regulation of megakaryocyte ploidy in vivo in the rat. Blood **75:**74–81.
25. **Lehner, C. F., and P. H. O'Farrell.** 1990. The roles of Drosophila cyclins A and B in mitotic control. Cell **61:**535–547.
26. **Lok, S., K. Kaushansky, R. D. Holly, J. L. Kuijper, C. E. Lofton-Day, P. J. Oort, F. J. Grant, M. D. Heipel, S. K. Burkhead, J. M. Kramer, L. A. Bell, C. A. Sprecher, H. Blumberg, R. Johnson, D. Prunkard, A. F. T. Ching, S. L. Mattewes, M. C. Bailey, J. W. Forstrom, M. M. Buddle, S. G. Osborn, S. J. Evans, P. O. Sheppard, S. R. Presnell, P. J. O'Hara, F. S. Hagen, G. J. Roth, and D. C. Foster.** 1994. Cloning and expression of murine thrombopoietin cDNA and stimulation of platelet production in vivo. Nature **369:**565–568.
27. **Manning, K. L., S. Novinger, P. S. Sullivan, and T. P. McDonald.** 1996. Successful determination of platelet lifespan in C3H mice by in vivo biotinylation. Lab. Anim. Sci. **46:**545–548.
28. **Matsushime, H., D. E. Quelle, S. A. Shurtleff, M. Shibuya, C. J. Sherr, and J.-Y. Kato.** 1994. D-type cyclin-dependent kinase activity in mammalian cells. Mol. Cell. Biol. **14:**2066–2076.
29. **Matsushime, H., M. F. Roussel, and C. J. Sherr.** 1991. Novel mammalian cyclins (CYL genes) expressed during G1. Cold Spring Harbor Symp. Quant. Biol. **56:**69–74.
30. **Mazur, E. M.** 1987. Megakaryocytopoiesis and platelet production: a review. Exp. Hematol. **15:**340–350.
31. **Nasmyth, K. A.** 1990. FAR-reaching discoveries about the regulation of START. Cell **63:**1117–1120.
32. **Odell, T. T., Jr., and C. W. Jackson.** 1968. Polyploidy and maturation of rat megakaryocytes. Blood **32:**102–110.
33. **Odell, T. T., C. W. Jackson, and R. S. Reiter.** 1968. Generation cycle of rat megakaryocytes. Exp. Cell Res. **53:**321–328.
34. **Owens, G. K.** 1989. Control of hypertrophic versus hyperplastic growth of vascular smooth muscle cells. Am. J. Physiol. **257:**1755–1765.
35. **Pines, J., and T. Hunter.** 1990. Human cyclin A is adenovirus E1A-associated protein p60 and behaves differently from cyclin B. Nature **346:**760–763.
36. **Quelle, D. E., R. A. Ashmun, S. A. Shurtleff, J. Y. Kato, D. Bar-Sagi, M. F. Roussel, and C. J. Sherr.** 1993. Overexpression of mouse D-type cyclins accelerates G1 phase in rodent fibroblasts. Genes Dev. **7:**1559–1571.
37. **Rao, S. S., and D. S. Kohtz.** 1995. Positive and negative regulation of D-type cyclin expression in skeletal myoblasts by basic fibroblast growth factor and transforming growth factor beta. A role for cyclin D1 in control of myoblast differentiation. J. Biol. Chem. **270:**4093–4100.
38. **Ravid, K., D. L. Beeler, M. S. Rabin, H. E. Ruley, and R. D. Rosenberg.** 1991. Selective targeting of gene products with the megakaryocyte platelet factor 4 promoter. Proc. Natl. Acad. Sci. USA **88:**1521–1525.
39. **Ravid, K., T. Doi, D. L. Beeler, D. J. Kuter, and R. D. Rosenberg.** 1991. Transcriptional regulation of the rat platelet factor 4 gene: interaction between an enhancer/silencer domain and the GATA site. Mol. Cell. Biol. **11:**6116–6127.
40. **Ravid, K., Y. C. Li, H. B. Rayburn, and R. D. Rosenberg.** 1993. Targeted expression of a conditional oncogene in hematopoietic cells of transgenic mice. J. Cell Biol. **123:**1545–1553.
41. **Sambrook, J., E. F. Fritsch, and T. Maniatis.** 1989. Molecular cloning: a laboratory manual, 2nd ed. Cold Spring Harbor Laboratory Press, Cold Spring Harbor, N.Y.
42. **Shivdasani, R. A., M. F. Rosenblatt, D. Zucker-Franklin, C. W. Jackson, P. Hunt, C. J. Saris, and S. H. Orkin.** 1995. Transcription factor NF-E2 is required for platelet formation independent of the actions of thrombopoietin/MGDF in megakaryocyte development. Cell **81:**695–704.

43. **Sicinski, P., J. L. Donaher, Y. Geng, S. B. Parker, H. Gardner, M. Y. Park, R. L. Robker, J. S. Richards, L. K. McGinnis, J. D. Biggers, J. J. Eppig, R. T. Bronson, S. J. Elledge, and R. A. Weinberg.** 1996. Cyclin D2 is an FSH-responsive gene involved in gonadal cell proliferation and oncogenesis. Nature **384:**470–474.
44. **Sicinski, P., J. L. Donaher, S. B. Parker, T. Li, A. Fazeli, H. Gardner, S. Z. Haslam, R. T. Bronson, S. J. Elledge, and R. A. Weinberg.** 1995. Cyclin D1 provides a link between development and oncogenesis in the retina and breast. Cell **82:**621–630.
45. **Stenberg, P. E., and J. Levin.** 1989. Ultrastructural analysis of acute immune thrombocytopenia in mice: dissociation between alterations in megakaryocytes and platelets. J. Cell. Physiol. **141:**160–169.
46. **Stenberg, P. E., J. Levin, and L. Corash.** 1990. Sustained thrombocytopenia in mice: serial studies of megakaryocytes and platelets. Exp. Hematol. **18:** 124–132.
47. **Thompson, A., Y. Zhang, D. Kamen, C. W. Jackson, R. D. Cardiff, and K. Ravid.** 1996. Deregulated expression of c-myc in megakaryocytes of transgenic mice increases megakaryopoiesis and decreases polyploidization. J. Biol. Chem. **271:**22976–22982.
48. **Tomer, A., L. A. Harker, and S. A. Burstein.** 1988. Flow cytometric analysis of normal human megakaryocytes. Blood **71:**1244–1252.
48a. **Toselli, P., B. Faris, D. Sassoon, B. A. Jackson, and C. Franzblau.** 1992. In-situ hybridization of tropoelastin mRNA during the development of the multilayered neonatal rat aortic smooth muscle cell culture. Matrix **12:**321–332.
49. **Ulich, T. R., J. del Castillo, G. Senaldi, O. Kinstler, S. Yin, S. Kaufman, J. Tarpley, E. Choi, T. Kirley, P. Hunt, and W. P. Sheridan.** 1996. Systemic hematologic effects of PEG-rHuMGDF-induced megakaryocyte hyperplasia in mice. Blood **87:**5006–5015.
50. **Ulich, T. R., J. del Castillo, S. Yin, S. Swift, D. Padilla, G. Senaldi, L. Bennett, J. Shutter, J. Bogenberger, D. Sun, B. Samal, G. Shimamoto, R. Lee, R. Steinbrink, T. Boone, W. T. Sheridan, and P. Hunt.** 1995. Megakaryocyte growth and development factor ameliorates carboplatin-induced thrombocytopenia in mice. Blood **86:**971–976.
51. **Vinci, G., A. Tabilio, J. F. Deschamps, D. Van Haeke, A. Henri, J. Guichard, P. Tetteroo, P. M. Lansdorp, T. Hercend, W. Vainchenker, and J. Breton-Goriun.** 1984. Immunological study of in vitro maturation of human megakaryocytes. Br. J. Haematol. **56:**589–605.
52. **Wang, Z., P. Sicinski, R. A. Weinberg, Y. Zhang, and K. Ravid.** 1996. Characterization of the mouse cyclin D3 gene: exon/intron organization and promoter activity. Genomics **35:**156–163.
53. **Wang, Z., Y. Zhang, D. Kamen, E. Lees, and K. Ravid.** 1995. Cyclin D3 is essential for megakaryocytopoiesis. Blood **86:**3783–3788.
54. **Wendling, F., E. Maraskovsky, N. Debili, C. Florindo, M. Teepe, M. Titeux, N. Methia, J. Breton-Gorius, D. Cosman, and W. Vainchenker.** 1994. cMpl ligand is a humoral regulator of megakaryocytopoiesis. Nature **369:**571–574.
55. **Yan, X. Q., D. Lacey, F. Fletcher, C. Hartley, P. McElroy, Y. Sun, M. Xia, S. Mu, C. Saris, D. Hill, R. G. Hawley, and I. K. McNiece.** 1995. Chronic exposure to retroviral vector encoded MGDF (mpl-ligand) induces lineage-specific growth and differentiation of megakaryocytes in mice. Blood **86:** 4025–4033.
56. **Zhang, Y., Z. Wang, and K. Ravid.** 1996. The cell cycle in polyploid megakaryocytes is associated with reduced activity of cyclin B1-dependent cdc2 kinase. J. Biol. Chem. **271:**4266–4272.
57. **Zucker-Franklin, D., and K. Kaushansky.** 1996. Effect of thrombopoietin on the development of megakaryocytes and platelets: an ultrastructural analysis. Blood **88:**1632–1638.
58. **Zwijsen, R. M. L., E. Wientjens, R. Klompmaker, J. van der Sman, R. Bernards, and R. J. A. M. Michalides.** 1997. CDK-independent activation of estrogen receptor by cyclin D1. Cell **88:**405–415.